

# Inverse methods for asteroid orbit computation.

Dagmara Oszkiewicz<sup>1</sup> and Karri Muinonen<sup>1,2</sup>

<sup>1</sup>University of Helsinki, <sup>2</sup>Finnish Geodetic Institute  
In collaboration with J.Virtanen, M. Granvik and T. Pieniluoma

ELSA conference 2010  
Gaia: at the frontiers of astrometry  
Sevres, 7-11 June 2010



# Asteroid orbital inverse problem

$y \in \mathbb{R}^m$  the measurements

$x \in \mathbb{R}^d$  the unknown parameters

To interpret the measurements we need to solve the inverse problem for  $x$ :

$$y = f(x) + \epsilon \quad (1)$$

The Bayesian solution:

$$p(x | y) = \frac{p(x)p(y | x)}{\int p(x)p(y | x)dx} \quad (2)$$

The posterior distribution combines a priori information  $p(x)$  and the measurement likelihood  $p(y | x)$ .

The Bayesian a posteriori p.d.f. of the orbital elements is given by:

$$p_p(\mathbf{P}) = C p_{pr}(\mathbf{P}) p_\epsilon(\Delta\Psi(\mathbf{P})), \quad (3)$$

- $p_{pr}(\mathbf{P})$  is the a priori p.d.f.
- $p_\epsilon(\Delta\Psi(\mathbf{P}))$  is observational error p.d.f., evaluated for the observed minus computed (O-C) residuals  $\Delta\Psi(\mathbf{P})$
- $C = (\int p(\mathbf{P}, \Psi) d\mathbf{P})^{-1}$  is the normalization constant
- $p(\mathbf{P}, \Psi) = p_{pr}(\mathbf{P}) p_\epsilon(\Delta\Psi(\mathbf{P}))$ .

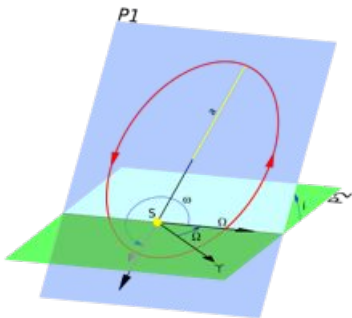


**Figure:**  $a$  - size of the orbit,  $e$  - describing the flatness,  $i$  - inclination with respect to the reference plane  $\Omega$ ,  $i$  - horizontally orients the ascending node, with the reference frame's vernal point,  $\omega$  - an angle measured from the ascending node to the semimajor axis.  $M$  - defines the position of the orbiting body along the ellipse at a specific time (the "epoch").

# MCMC ranging

## Markov-Chain Monte-Carlo ranging (MCMC):

- Choose two observations  $A$  and  $B$  from  $\psi$ . Pick  $p_t$  for the topocentric spherical coordinates at the two observation dates  $A$  and  $B$  (e.g simple 6D gaussian in spherical coordinates phase space = complicated  $p_t$  in orbital-elements phase space)
- Propose new candidate orbit with the help of proposal densities,
- Accept or reject the orbit as a new sample, based on  $a_r$

$$a_r = \frac{p_p(\mathbf{P}')}{p_p(\mathbf{P}_t)} \frac{p_t(\mathbf{Q}_t, \mathbf{Q}') J_t}{p_t(\mathbf{Q}', \mathbf{Q}_t) J'}, \quad (4)$$

where  $J'$  and  $J_t$  are the determinants of Jacobians from topocentric coordinates to orbital parameters for the candidate and the last accepted sample, respectively.

Acceptance criteria:

If  $a_r \geq 1$ , then  $\mathbf{P}_{t+1} = \mathbf{P}'$ .

If  $a_r < 1$ , then  $\begin{cases} \mathbf{P}_{t+1} = \mathbf{P}', & \text{with probability } a_r, \\ \mathbf{P}_{t+1} = \mathbf{P}_t, & \text{with probability } 1 - a_r. \end{cases}$

- Repeat many times to reach the stationary distribution.

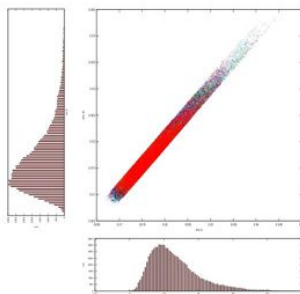


**Figure:** Distribution of ranges for the 2099 DD<sub>45</sub>, assuming 2.0 arcsec observational error. Colors correspond to different Markov chains.

## Convergence diagnostics

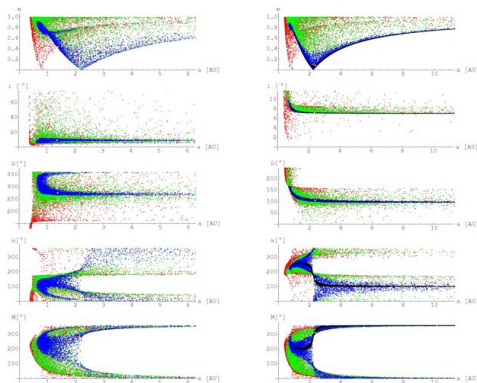
relates to the idea that Markov chain after sufficient number of iterations will eventually converge to the stationary distribution (target distribution), starting from any point in the phase-space and then mix in that phase-space forever.

## Other convergence diagnostics based on:

- Different approaches single vs. many chains
- Shrink factor (Gelman and Rubin, 1992)
- Autocorrelation function
- Running means of parameters (Gewke, 1992)
- Marginal probability plots
- Others (comparative review can be found in e.g. Cowles and Carlin, 1996)



# Applications and examples



Sets of distributions each composed of 5000 possible orbit solutions for the near-Earth objects (1685) Toro (left), (4) Vesta (right) obtained from simulated Gaia data. The distributions were obtained using 3 observations from a single scan (observational time interval of 0.25 d) - Toro, 4 observations (observational time interval of 0.32 d) - Vesta.

More in: "Asteroid orbits with Gaia using Markov-Chain Monte-Carlo ranging", D.Oszkiewicz, K.Muionen, J.Virtanen, M.Granvik, 1st IAA Planetary Defense Conference: Protecting Earth from Asteroids, proceedings.

We contribute to the Gaia processing pipeline - CU4/DU456.

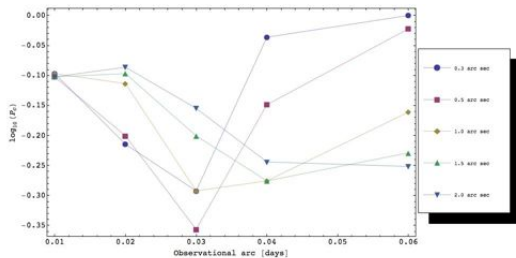


**Figure:** Time evolution of collision probabilities for 2008 TC<sub>3</sub> using MCMC ranging generated orbits with Jeffreys apriori (n-body approach).

Nr. of obs.	Noise [arcsec]:	MCMC ranging: Jeffrey's apriori
2	0.3	0.80 (15281)
	0.5	0.79 (15114)
	1.0	0.80 (14584)
	1.5	0.79 (13991)
	2.0	0.79 (13585)
3	0.3	0.61 (2813)
	0.5	0.63 (3271)
	1.0	0.77 (6025)
	1.5	0.80 (8412)
	2.0	0.82 (12113)
4	0.3	0.51 (14960)
	0.5	0.44 (7878)
	1.0	0.51 (4742)
	1.5	0.63 (6116)
	2.0	0.70 (8678)
5	0.3	0.92 (44053)
	0.5	0.71 (28966)
	1.0	0.53 (12620)
	1.5	0.53 (9611)
	2.0	0.57 (8930)
6	0.3	$\approx 1.0$ (49771)
	0.5	0.95 (46079)
	1.0	0.69 (27786)
	1.5	0.59 (16348)
	2.0	0.56 (11939)

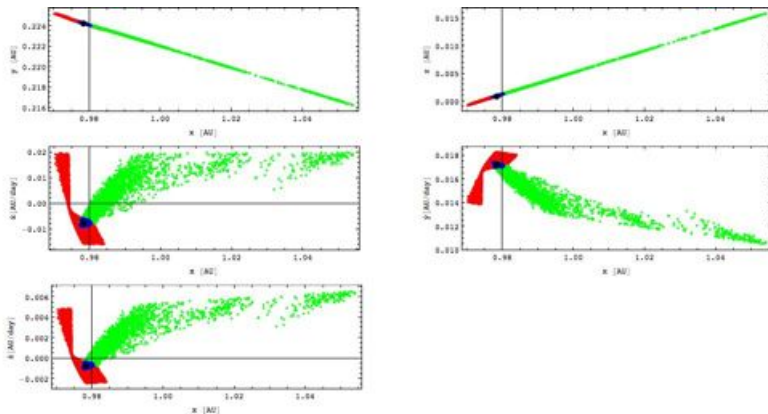


**Figure:** (a) Green - marginal distribution of orbital elements obtained for asteroid 2008 TC3 using 5 observations and 0.5 arcsec noise assumption. Blue - orbits leading to a collision with the Earth from the green set. Red - orbits leading to a collision with Earth obtained using 3 observations and 2.0 arcsec astrometric noise assumption.

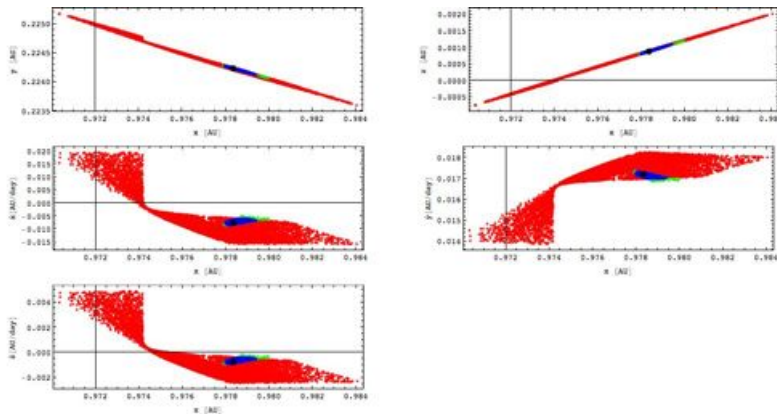


**Figure:** (b) Green - marginal distribution of orbital elements obtained for asteroid 2008 TC3 using 6 observations and 0.3 arcsec noise assumption. Blue - orbits leading to a collision with the Earth from the green set. Red - orbits leading to a collision with Earth obtained using 3 observations and 2.0 arcsec astrometric noise assumption.

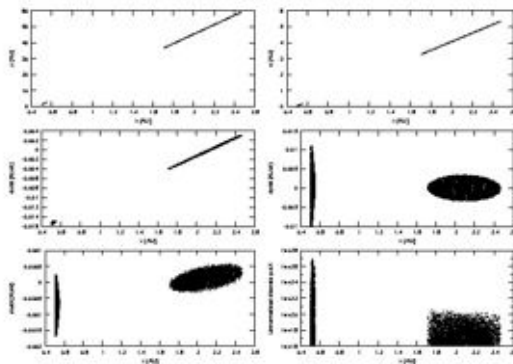


**Figure:** Cartesian orbital-element PDF for 2003 WW<sub>188</sub>. Although a TNO solution is possible, an NEO solution is more likely. However, since the observational time span is only about three days and the number of observations is three, one should not draw too definite conclusions either way.

## Summary:

- We have developed novel variants of asteroid orbit computation methods that map the extensive volume of solution space.
- Distribution of O-C residuals could be used as outlier detection criteria.
- These methods can also be useful in other problems like computing collision probabilities, dynamical classification, performing the recovery of lost objects.



## Poster number 15!

## Asteroid spin and shape inversion for simulated Gaia photometry

Dagmara Oszkiewicz<sup>1</sup>, Karri Muinonen<sup>1,2</sup> and Tuomo Pieniluoma<sup>1</sup><sup>1</sup> Department of Physics, P.O. Box 64, FI-00014 University of Helsinki, Finland  
<sup>2</sup> Finnish Geospatial Institute, P.O. Box 16, FI-00023 Mikkola, Finland

## Introduction

While determining and cataloguing astrometric positions and movements of about one billion stars, Gaia will observe some hundreds of thousands of asteroids [1]. Photometric data of asteroids will consist of single brightness values ranging over a time interval of five years. This results in a maximum of about one hundred brightness values at varying observing geometries. Here we apply Markov-chain Monte-Carlo methods [2] to simulated asteroid data in order to obtain spins and shapes of the simulated asteroids (for conventional convex inverse methods, see [3] and [4]). The inverted and original shape and spin solutions are compared to validate the applicability of the methods to the Gaia data.

## MCMC sampling

We make use of general convex shapes described using a large but finite number of triangles with or without smoothing using barycentric splines. In MCMC convex inversion, the convex shape solutions are directly sampled. There are four parameters for the spin characteristics: the rotational period, the ecliptic longitude and latitude of the rotational pole, and the rotational phase of the object at a given time. The 3D Cartesian coordinates of the  $N$  triangle nodes constitute the free shape parameters. Altogether, there are  $4 + 3N$  free parameters [2]. In MCMC convex inversion, the inversion parameters are sampled according to the Metropolis-Hastings algorithm [5]. The accepted shapes and spins generate a sequence of Markov chains. The proposed spin and shape parameters are accepted or rejected depending on a posterior probability density value corresponding to the proposed and current parameters. If the proposed parameters provide a better fit to the data than the current, they are always accepted. If not, they are accepted with a certain probability.

## Simulated Gaia photometry

The data was generated for a Gaiaian sample sphere mimicking an asteroid. The observing geometries were those simulated for asteroid lists for the five-year mission duration [6]. The data for Vega amounts to 69 simulated data. The accuracy of the brightness data was 0.01 mag.

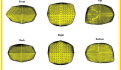
## [21] Lutetia data

We have also applied the method to [21] Lutetia which is an M-type, main-belt asteroid (about 100 km in diameter). [21] Lutetia will be the object of a flyby (11 July 2010) by the Rosetta space probe on its way to the comet 67P/Churyumov-Gerasimenko. Here we make use of the 26 lightcurves, making the total of 1126 photometric observations over a period of 20 years, 3 months and 26.56 days from the Standard Asteroid Photometric Catalogue (SAPC) – (<http://asteroid.astro.helsinki.fi/>).

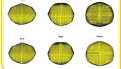
## Shape



Above: Original shape used to simulate Gaia data. Below: Shape inverted from the simulated photometric Gaia data using convex stochastic optimization. The best fit resulted in an  $m$ -value of 0.02. In inversion, three triangle nodes were utilized per cent.



Overall the shapes are in agreement, but the local valleys and hills are hidden. Below: Shape inverted from the photometric lightcurves of asteroid [21] Lutetia using convex stochastic optimization.



## Conclusions

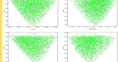
We have applied convex stochastic optimization and MCMC inversion methods to derive asteroid spins and shapes using simulated Gaia photometry. The original and inverted shapes are overall in good agreement. The local features are not reflected in the inverted shape. MCMC asteroid lightcurve inversion methods can potentially be applied to the forthcoming asteroid photometric observations by the Gaia mission [4] or the lightcurves stored in Standard Asteroid Photometric Catalogue (<http://asteroid.astro.helsinki.fi/>).

## References

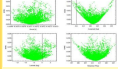
- [1] K. Muinonen, M. T. Jurgens, A. Deller, and T. J. van den Broek. Rotational properties of asteroids from Gaia data: simulated photometry. *A Space Agency*. In *Asteroids III*, pp. 200–209 (2006).
- [2] D. Oszkiewicz, D. Kucharski, and M. T. Jurgens. Lightcurves, lightcurves, and lightcurves. *International Asteroid Symposium*, pp. 104–108 (2006).
- [3] T. J. van den Broek, D. Kucharski, A. Deller, and K. Muinonen. Shape and rotational properties of binary asteroids from photometric data. In *Small Sat. III*, pp. 100–103 (2006).
- [4] D. Oszkiewicz, T. Jurgens, and K. Muinonen. Optimization methods for asteroid lightcurve inversion. In *The complete inverse problem*. In *Planet. Space Sci.*, pp. 17–19 (2007).
- [5] R. G. Gelman, A. Geweke, and J. S. Vehtari. *Markov Chain Monte Carlo in Practice*. Chapman and Hall/CRC (1996).
- [6] T. Jurgens and K. Muinonen. Statistical inversion of Gaia photometry for asteroid spins and shapes. In *Three Dimensional Inverse with Gaia*, ESA Special Publication SP-1571 (1). Tassan, R., S. Pálffy, and M. A. C. Perryman, Eds., ESA Publications Division (2008). The Netherlands, pp. 103–109 (2008).

## Rotational period and pole

Below: Rotational period and pole distributions as obtained from MCMC convex inversion for the simulated Gaia data. Original spin parameters: rotation period 10.7795(273), ecliptic longitude of rotational pole 62.89 deg, ecliptic latitude of rotational pole 62.89 deg, rotational phase 131.1 deg.



Below: Rotational period and pole distributions around one of the possible poles obtained from MCMC convex inversion for asteroid [21] Lutetia. Here we used 100 chains and 50 samples in each chain. We utilize a two-dimensional proposal pdf. For the optimal pole combination with mean 1.0 deg and standard deviation of 0.1 deg. The proposal standard deviation for the period is 10<sup>-3</sup> h. The shape model contained 4 triangle nodes per cent.



Torges et al. [5] list two pole solutions for [21] Lutetia:  $\lambda_1 = 63$  deg,  $\beta_1 = 39$  deg,  $\phi_1 = 13$  deg,  $\lambda_2 = 220$  deg, a rotational period of  $P = 9.845453$  hrs, obtaining the best fit  $m$  value. This is in accordance with our estimate.

